# We are IntechOpen,
# the world's leading publisher of Open Access books
# Built by scientists, for scientists

## 4,800
Open access books available

## 122,000
International authors and editors

## 135M
Downloads

## 154
Countries delivered to

Our authors are among the

## TOP 1%
most cited scientists

## 12.2%
Contributors from top 500 universities

**BOOK CITATION INDEX**
CLARIVATE ANALYTICS
INDEXED

**WEB OF SCIENCE™**

Selection of our books indexed in the Book Citation Index
in Web of Science™ Core Collection (BKCI)

# Interested in publishing with us?
# Contact book.department@intechopen.com

Numbers displayed above are based on latest data collected.
For more information visit www.intechopen.com

# Isotopic Application in High Saline Conditions

*Minghui Li, Xiaomin Fang, Jiao Li, Maodu Yan, Shurui Sun and Liping Zhu*

## Abstract

Evaporite minerals record the hydrogeochemical conditions in which they precipitated. And therefore they can be used to reconstruct the paleoclimate and paleoenvironments. Evaporite minerals are also major sources of industrial minerals including gypsum, halite, borates, lithium concentrates, and others. Because of their scientific significance and economic importance, evaporite minerals and their isotopic hydrochemical processes linked to their formation have been the focus of many geologists and paleoclimatologists. This chapter will discuss the application of isotopes of hydrogen, oxygen, sulfur, strontium, and boron in saline conditions. This will include the following: the $\delta^{18}O$ and $\delta D$ of hydrated water of gypsum and their paleoclimate since 2.2 Ma in the Qaidam Basin, NE Tibetan Plateau; the $\delta^{18}O$ and $\delta D$ of the interlayer water of clay minerals in salar lacustrine sediments; and the $^{87}Sr/^{86}Sr$, $\delta^{34}S$, and $\delta^{11}B$ of halite from evaporite deposits in Khorat Plateau, Laos, and Yunnan and their application in the origins of brine.

**Keywords:** oxygen and hydrogen, Sr isotope, sulfur isotope, boron isotope, salt minerals

## 1. Introduction

Evaporite minerals record the hydrogeochemical conditions in which they precipitated. And therefore they can be used to reconstruct the paleoclimate and paleoenvironments. Evaporite minerals are also major sources of industrial minerals including gypsum, halite, borates, lithium concentrates, and others. Given their scientific significance and economic importance, evaporite minerals and their isotopic hydrochemical processes linked to their formation have become the focus of many geologists and paleoclimatologists. The Qaidam Basin and Lanping-Simao Basin (LSB) in China and Khorat Basin (KB) and Sakhon Nakhon Basin (SNB) in Thailand and Laos, which have thick sequences of evaporites, have been the focus of study by researcher concerned with its mineral resources, geochemistry, paleoenvironmental evolution, and tectonic uplift [1–3].

Water is nearly ubiquitously in nature. Its isotopic compositions also were recorded in many minerals. In order to identify the past conditions at which sediments formed, many studies focused on the stable isotopes of carbon and oxygen as tracers of environmental conditions. However, we know little about the $\delta^{18}O$ and $\delta D$ in saline conditions. On the other hand, halite and gypsum are two common minerals in evaporite deposits. Today, exploited evaporite deposits are most found

in the arid and semiarid deserts of the world (the areas between latitudes 15° and 45° both north and south of the equator). Tectonics, climate, and origins of brine are the prime controls on most evaporite deposits. However, the origins of brine was a big topic for some giant evaporite deposits, for example, the evaporite deposit in Khorat Basin (KB) in Thailand, Sakhon Nakhon Basin (SNB) in Laos, and Lanping-Simao Basin (LSB) in China. Almost all large potash deposits are associated with marine fluids (such as the deposits in Thailand, the United States, Germany, Russia, France, and Brazil), whereas some small potash deposits are with fluids of continental source (such as deposits in the Qaidam Basin, Western Tibet, China) [1, 2]. The isotopes of S, Sr, and B of halite could be very useful in determining the origins of brine. So this chapter will use well-known accepted methods to analyze minerals (halite, gypsum, and clay minerals) and stable isotopes ($\delta^{18}O$ and $\delta D$, $^{87}Sr/^{86}Sr$, $\delta^{34}S$, and $\delta^{11}B$) to discuss their application in paleoclimate and origins of brine.

## 2. The $\delta^{18}O$ and $\delta D$ in saline conditions

### 2.1 Geological setting and the Core SG-1 in the Qaidam Basin, NE Tibetan Plateau

The Qaidam Basin is a Mesozoic-Cenozoic sedimentary basin located on the northern margin of the Tibetan Plateau in China (**Figure 1**). The Asian inland drought basin was formed as the result of intracontinental deformation and plateau uplift due to the collision of the Indian and Eurasian Plates. It is bordered by the Kunlun Mountains to the south, the Qilian Mountains to the northeast, and the Arjin Mountains to the northwest, which have altitudes ranging from 4000 to 4500 m asl to over 5000 m asl. A network of faults exists within the basin [3]. The Paleogene and Neogene strata are widespread and include intrusive rocks. From the Middle Oligocene to the Upper Pliocene, the strata consist of mudstones, calcareous mudstones and marls, intercalating siltstone, very thick gypsum, and rock salt beds in the western basin [4]. Some secondary or subsidiary basins have become well developed since the Middle Pleistocene as a result of slow uplift [1]. Lacustrine sediments in
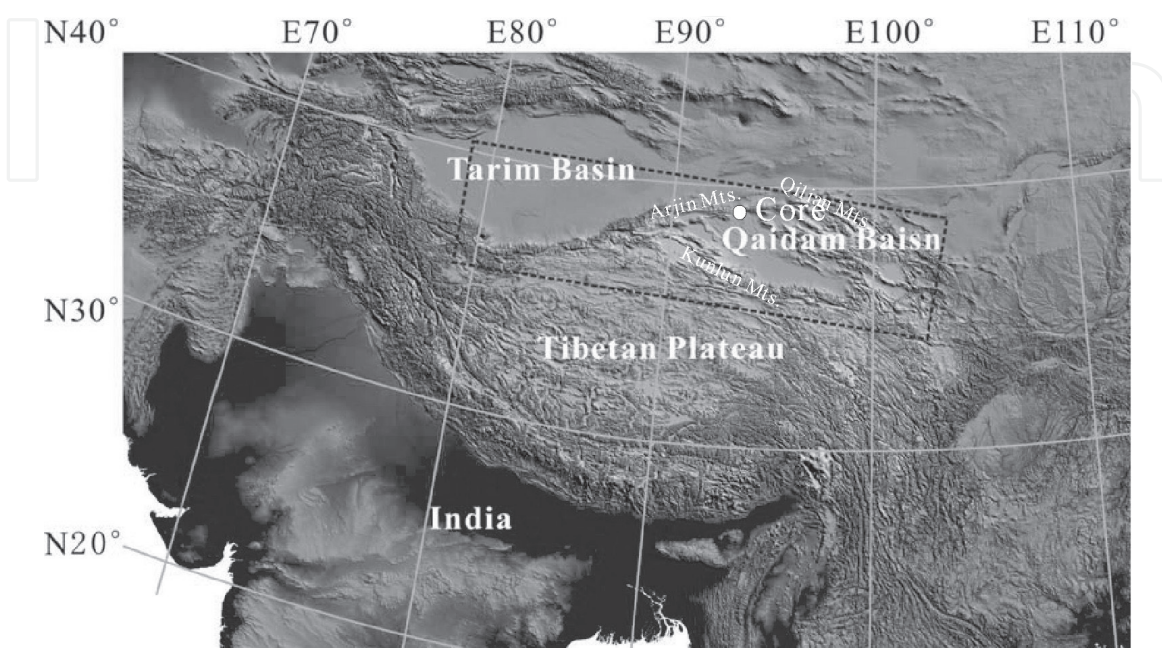


**Figure 1.**
*Map of the Qaidam Basin showing the core site.*

the basin cover an area of 30,000 km$^2$ with strata up to 700 m thick [4]. Abundant records of palaeo-lake level and paleoclimatic changes are indicated by various proxies, such as pollen, ostracods, evaporite minerals, and isotopic geochemistry [5, 6]. Studies on evaporite minerals and hydrochemistry and geochemistry of salt lakes have been ongoing for about 50 years because of great economic significance [1, 2, 5, 7]. However, no two drainage basins have identical climatic and hydrologic conditions, and even adjacent basins can show striking variations in evaporite mineralogy [8].

The Core SG-1 (38°24'35.3" N, 92°30'32.7" E, 2900 m asl) was located in a playa in the Qahansilatu sub-basin, western Qaidam Basin (**Figure 1**). The core spanned from 2.77 to 0.1 Ma, dated by paleomagnetism and optically stimulated luminescence (OSL) with a sedimentary rate of 26.1–51.5 cm/ka [9]. The sedimentary sequence is composed of clay, clay-silt, and siltstone intercalated with salt layers (mainly halite), marl beds, and thin and/or scattered gypsum crystals, indicating clay-silt and halite-marl depositional cycles (**Figure 2**). The fluctuation between evaporite minerals and carbonaceous clay strata indicates a shift between dry and wet climates. Gypsum and halite make up the majority of the evaporite minerals in the core [11, 12]. During the last ~2.8 Ma, the lake basin evolved from a semi-deep fresh lake to a semi-brackish lake (2.8–2.2 Ma), to a perennial saline lake (2.2–2.0 Ma), to a shallow brackish lake (1.8–1.6 Ma), to a perennial saline lake (1.2–0.6 Ma), to a playa saline lake (0.9–0.6 Ma), and to a saline mudflat (0.6–0.1 Ma) [10] (**Figure 2**). Multi-proxies, such as sedimentary features [10], salt minerals [11], isotope records [13, 14], and rare earth elements [15] of the study area, indicate the long-term persistent aridification of inland Asia since 2.8 Ma.

## 2.2 Clay minerals and the δ$^{18}$O and δD of their interlayer water

### 2.2.1 Clay minerals

Clay minerals have been used to reconstruct paleoclimates and environments since Singer's review in 1984 [16]. It is common that the clay minerals undergo
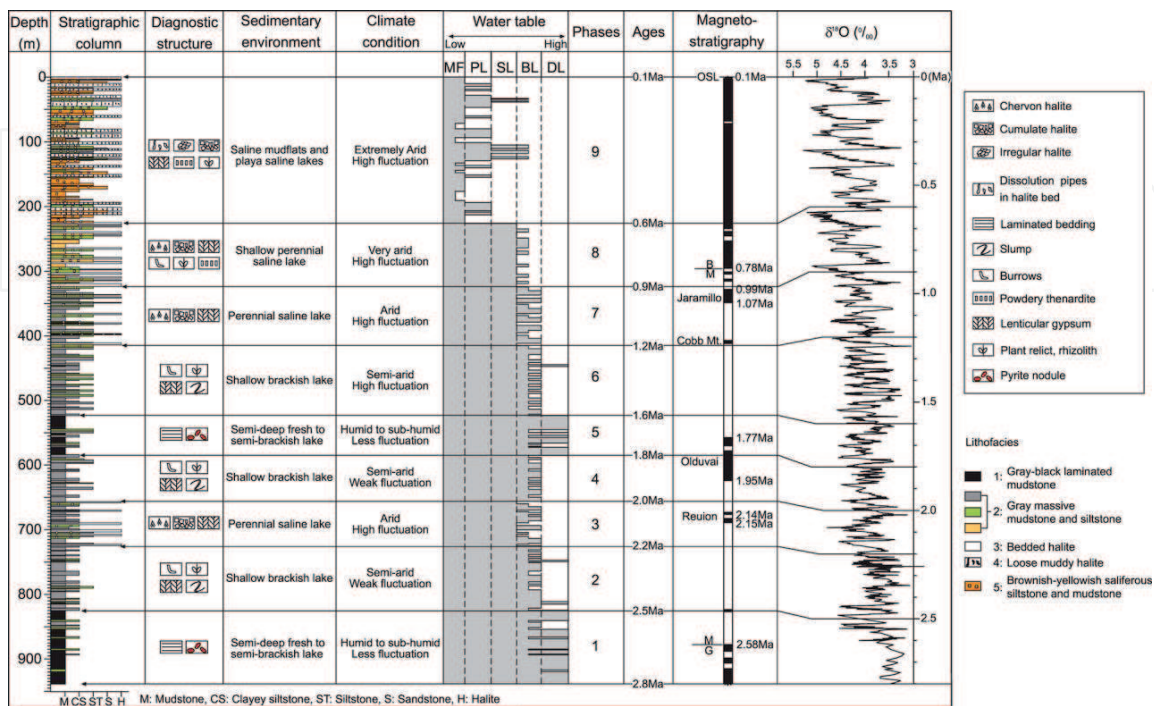


**Figure 2.**
*Lithology, sedimentary environment, sediment accumulation rates (SAR), and magnetostratigraphic ages of the Core SG-1 (after Zhang et al. [9] and Wang et al. [10]). DL, semi-deep fresh to semi-brackish lake; BL, shallow brackish lake; SL, perennial saline lake; PL, playa saline lake; and MF, playa saline mudflat.*

diagenetic transformations or postdepositional diagenetic changes, and as a result, some paleoclimate information of clays will be overprinted or changed. However, there are still lots of studies to use clay minerals to reconstruct paleoenvironments and paleoclimates. The isotopic exchange rates between the interlayer water of clay minerals and the ambient water are very fast and, in general, are less than a few days. However, in saline conditions, we know little about the isotopic exchange between them.

The clay mineral assemblages in the Core SG-1 are shown in **Figure 3**. The curves of chlorite and illite abundances are similar, but they are different with those of the kaolinite, smectite, and I/Sm (**Figure 3**). The curve of smectite content shows a decreasing trend with decreasing depth, and that of the illite content shows an increasing trend slightly (**Figure 3**). The XRD analyses suggest that the I/Sm in the core exhibits order ($R_3$ I/Sm) (mixed layer of I/Sm > 80%). $R_1$ I/Sm is more stable than any other mixed layer I/Sm phase because it has a unique structure, composition, and order [17]. The clay minerals that were identified as $R_3$ I/Sm by XRD analyses are possible to be mixtures of discrete smectite and $R_1$ I/Sm [17].

The diagenesis of clay minerals in lacustrine sediments is a disputed topic. The clays in Core SG-1 in the Qaidam Basin probably underwent early diagenesis based on their curves and relationship between them (**Figures 4** and **5**) [18]. Climate changes, to some extent, control on the degree of alteration of the primary minerals and the composition of the secondary products. In the clay minerals, the exchange between the interlayer water and the ambient water recorded the diagenetic information. For instance, the $\delta^{18}O$ and $\delta D$ of the different clays and interlayer water record temperatures that range from surface temperatures to hydrothermal temperatures of about 150–200°C [19]. In situ precipitation of I/Sm minerals may take place in chemical and isotopic equilibrium with the reacting solution [20, 21]. However, in high saline conditions, the reaction or the above exchange may be extremely slowly.

### 2.2.2 The $\delta^{18}O$ and $\delta D$ of the interlayer water

The $\delta^{18}O$ of the interlayer water ranged from −11.8 to 82.95% with the average of 20.8%, and the $\delta D$ ranged from −114.3 to 165.5% with the average of −35.6%
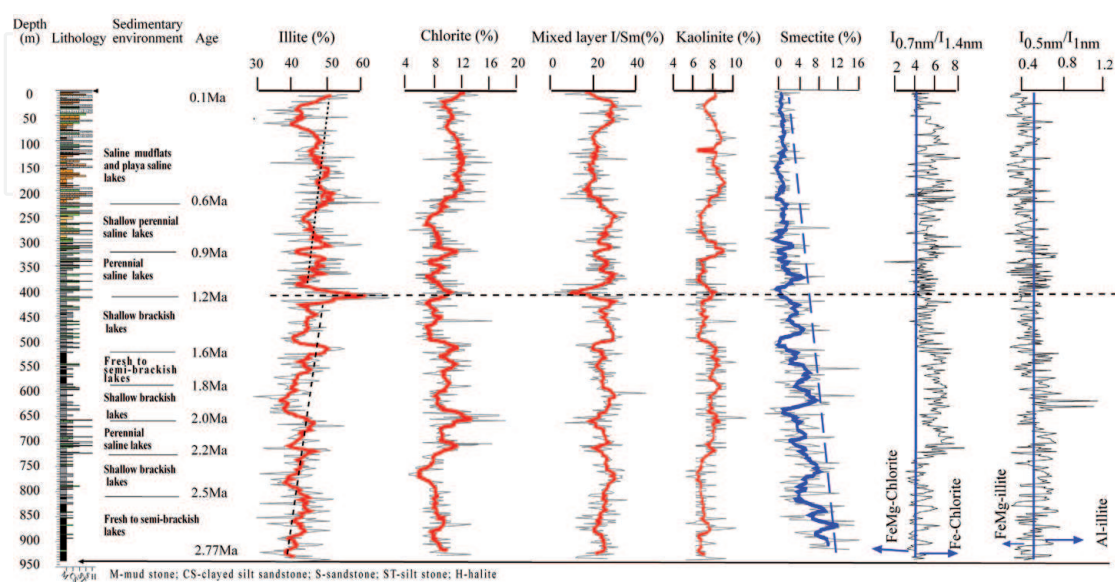


**Figure 3.**
*Variations in the amount of illite, chlorite, kaolinite, smectite, and illite/smectite (I/Sm) and in the chemistry of illite (I5Å/I10Å ratios) and chlorite (I7Å/I14Å ratios). Colored lines represent a five-point running average. Sedimentary environments are from Wang et al. [10]; ages are from Zhang et al. [9].*
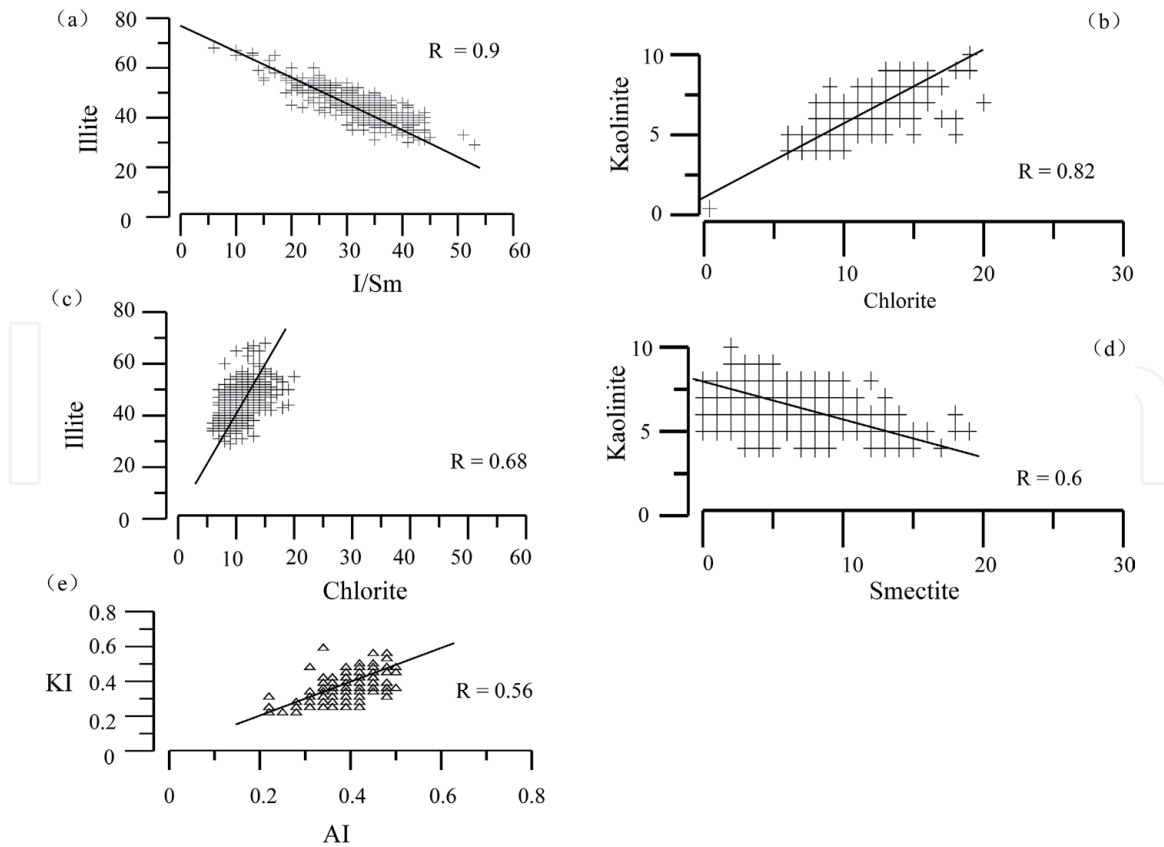
**Figure 4.**
*Correlations between the abundances (%) of (a) illite and I/Sm, (b) chlorite and kaolinite, (c) illite and chlorite, (d) smectite and kaolinite, (e) KI (Kübler index), and AI (Árkai index).*
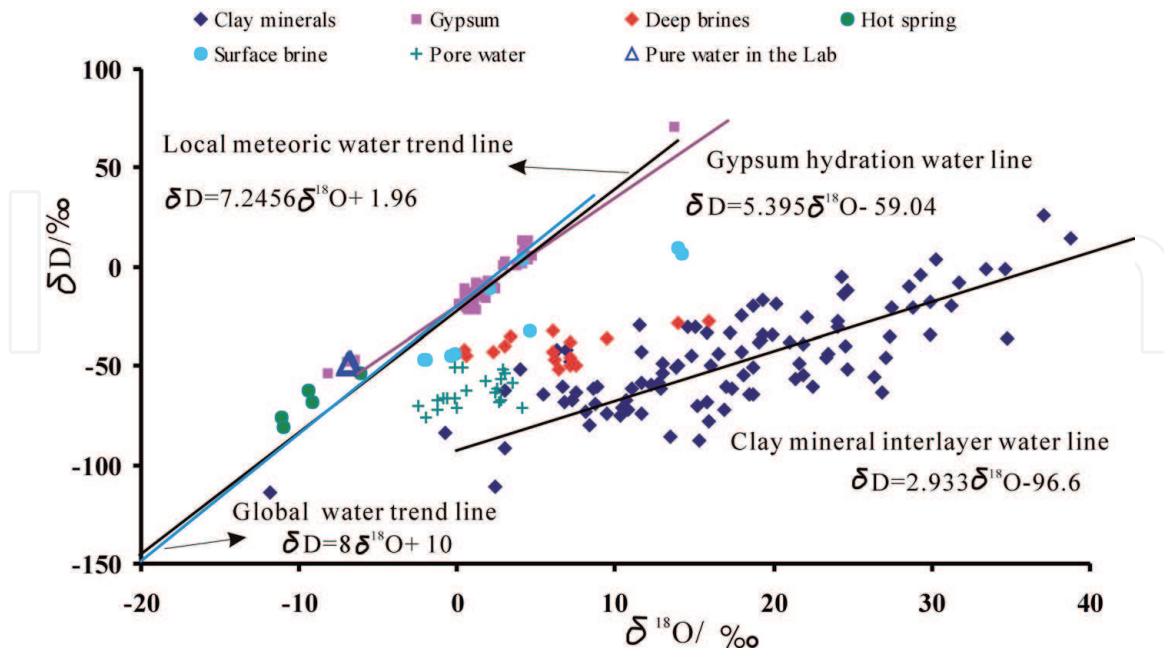


**Figure 5.**
*Relationship between the $\delta^{18}O$ and $\delta D$ of the interlayer water of the clay minerals and different types of water from the Qaidam Basin. The global and modern local meteoric water lines are from Craig [22] and Li et al. [23], respectively. The present-day precipitation and hot spring data are from Zhang [24]. Gypsum hydration water data are from Li et al. [14], deep brine water data are from Fan et al. [25], and surface water and pore water data are from Xiao [26] and Fan et al. [25]. The large differences in the $\delta^{18}O$ and $\delta D$ of the pure water and the interlayer water of the clay minerals suggest that the interlayer water did not exchange with the pure water and other water used during the processing and pretreatment.*

(**Figure 5**). They exhibit a roughly linear relationship and are significantly correlated ($R = 0.96$), indicating that these isotopes share the same sources. The isotopes of the interlayer water possibly recorded the brine composition which contained interstitial water or pore water derived from lake water and underwent strong evaporation. This could be understood as the following. (a) Some of the $\delta^{18}O$ and $\delta D$ of the interlayer water are close to those of surface water, deep brine, and pore water. (b) The rates of isotopic exchange between the interlayer water and the ambient water are very fast and, sometimes, are less than a few days. Therefore, the exchange rate between the structural oxygen of the clay minerals and that of the ambient water could be insignificant over a 2.8 Ma time span at a temperature of $\leq 100°C$ [27, 28]. (c) The slopes of the $\delta^{18}O$ and $\delta D$ of the interlayer water are smaller than that of the gypsum hydrated water that recorded the evolution of lake water or subsurface water (**Figure 5**), suggesting the interlayer water underwent more stronger evaporation than gypsum hydrated water. (d) The $\delta^{18}O$ and $\delta D$ of the interlayer water of clay minerals are very different with those of pure water (**Figure 5**), which was used to treat the clay minerals.

Independent of the oxygen isotopic exchange, the hydrogen isotopic exchange occurs by a proton exchange mechanism [28, 29]. The hydrogen isotopic exchange between smectite and its ambient water is very fast and significantly relative to that between illite and kaolinite with their ambient water [28].

## 2.3 Gypsum and the $\delta^{18}O$ and $\delta D$ of hydrated water

### 2.3.1 Gypsum

Gypsum ($CaSO_4 \cdot 2H_2O$), one of the most abundant evaporite minerals occurring as a syndepositional evaporite, carries information about brines from which they precipitate. There are several shapes of gypsum crystals (**Figure 6**). These prismatic and tabular gypsum layers were vertically aligned, indicating primary subaqueous precipitates and with bottom nucleation [31, 32]. Some euhedral gypsum crystals were scattered in the mudstone-siltstone layers, which are possibly formed by evaporation of pore water or interstitial brine and regarded as diagenetic gypsum. Based solely on their morphology, it is not easy to confirm gypsum to be synsedimentary or diagenetic, because there is no diagnostic relationship between crystal morphology and depositional environment [33]. Besides the aligned gypsum, scattered euhedral crystals may be significant for understanding the evolution of lake water, because pore water or interstitial brine may have originated from infiltration of lake water. The Core SG-1 showed an increase of evaporite mineral contents upward, and the strata were mainly horizontal and not affected by tectonic deformation [10]. Therefore, these selected gypsums may have been primary in origin in arid, or aqueous, young lacustrine. These environments contain deposits that have never been exposed or deeply buried and may also retain their original isotopic compositions [34–36].

Minor cations such as $Sr^{2+}$, $K^+$, and $Mg^{2+}$ may be incorporated into gypsum lattice via substitution for $Ca^{2+}$ during the coprecipitation process because they have similar ionic radii. Different cations are selectively attracted to particular faces [37, 38]. For example, the (1 1 1) face is covered by either calcium ions or sulfate clusters and the (1 1 0) and (0 1 0) faces by both calcium and sulfate clusters [39]. $Na^+$ is preferentially adsorbed on (1 1 1) surface of sulfate salts that is dominantly occupied by $Ca^{2+}$ [39, 40]. However, the presence of $Na^+$ also impedes the (1 1 1) face growth and, as a result, minimizes parallel to its c axis [36, 39]. $K^+$ has a similar inhibitory effect [40]. Because of the difference in coordination number between $Ca^{2+}$ (eight in gypsum) and $Mg^{2+}$ (six in most minerals), $Mg^{2+}$ will disturb gypsum
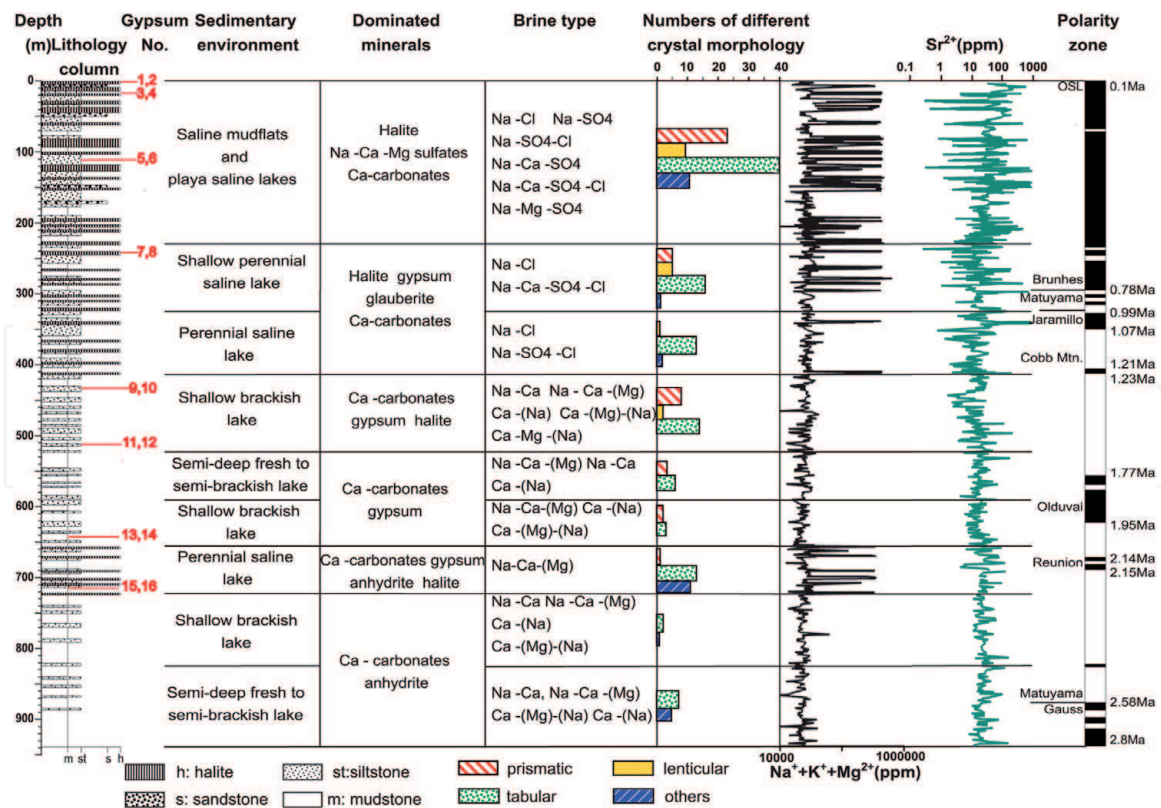
**Figure 6.**
*The monoclinic gypsum exhibits four principal forms in the Core SG-1 [30]: prismatic crystals, lenticular crystals, and tabular crystals. The tabular and prismatic crystals tend to increase with decreasing depth. The red numbers mean that the same kind of crystal morphology can appear in different environments and different crystal morphologies can also occur in the same depositional environment.*

growth along c axis [41]. Preferentially adsorbed on the (1 1 0) face, $Sr^{2+}$ forms epitaxial deposits of strontium sulfate [39]. Therefore, $K^+$, $Na^+$, and $Mg^{2+}$ make the c value smaller, while $Sr^{2+}$ reduces a and b values. As a result, there have different gypsum morphologies.

### 2.3.2 The $\delta^{18}O$ and $\delta D$ of hydrated water

The $\delta^{18}O$ of gypsum hydrated water ranged from −4.21 to 8.69%, with average of 5.74%; and the $\delta D$ was from −72.77 to 49.73%, with average of −28.09%. They exhibit a roughly linear relationship with the slope of 5.39, and its mother water-line has a slope of 5.52 (**Figure 7**). The $\delta^{18}O$ and $\delta D$ appear to be much lower than those of today's mean precipitation ($\delta^{18}O$ = −9.25% and $\delta D$ = −41.3%) [14]. This indicated a slightly weaker evaporation and/or colder climate than today [36, 43]. On the other hand, the $\delta^{18}O$ and $\delta D$ are close to those of the Altyn Tagh Mountain groundwater that sourced from meteoric water (**Figure 7**). It is therefore likely that meteoric water was the main source of hydration water during gypsum formation.

In general, gypsum could be formed in the following ways: in situ formation (e.g., resulting from the oxidation of sulfide minerals); hydration of anhydrite; and direct deposition from an evaporating solution saturated with gypsum [44]. If gypsum was formed in situ formation, the $\delta^{18}O$ and $\delta D$ of hydrated water would reflect those of meteoric and/or surface waters [44, 45]. If it is formed from the hydration of anhydrite, which is assumed to be a Rayleigh process, both the hydration water and its mother water would be expected to move along a line with a negative $\Delta\delta D/\Delta\delta^{18}O$ [46, 47]. In this study, the $\Delta\delta D/\Delta\delta^{18}O$ value was 5.39 [14], suggesting evaporation to be the major geochemical process for gypsum deposition, that is, the gypsum in the Core SG-1 was likely to deposit directly from brines. The degree
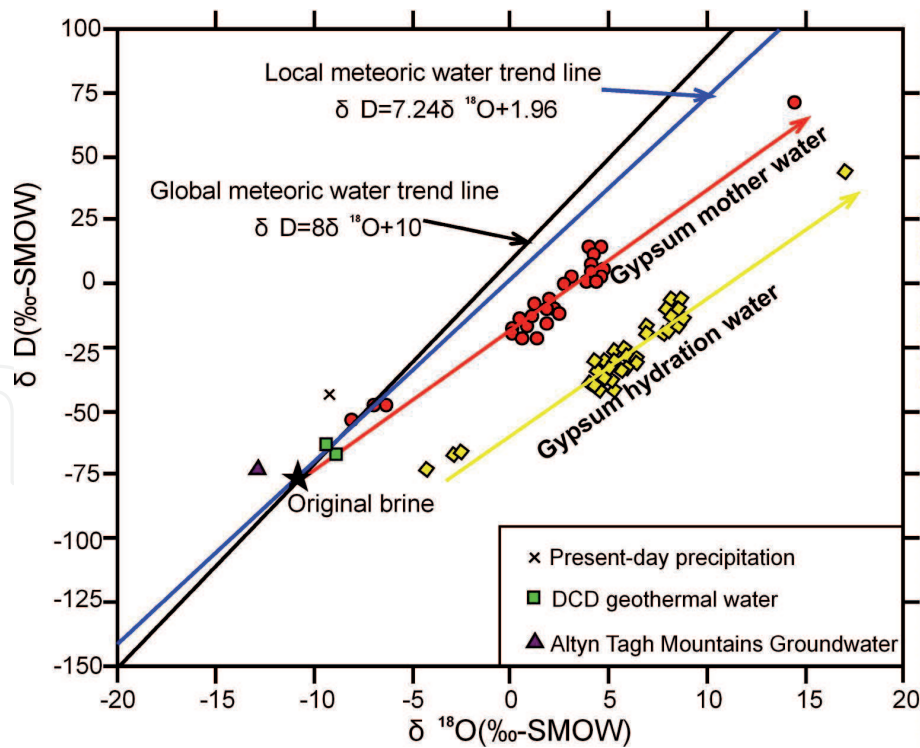
**Figure 7.**
*Relationship between $\delta^{18}O$ and $\delta D$ of gypsum hydration water and mother water as compared to meteoric water and different types of water from the Qaidam Basin. The global and modern local meteoric waterlines are from Craig [22] and Li et al. [23], respectively. The present-day precipitation and Dachaidan geothermal water are from Zhang [24]. Altyn Tagh Mountain groundwater data are from Wang et al. [42].*

of evaporation depends upon the salinity and atmospheric humidity [22, 48]. In humid conditions, $\Delta\delta D/\Delta\delta^{18}O$ gradients are usually between ~5 and ~6, whereas the gradient can be low as 2.5–4 in arid regions. The evaporation line gradient for present-day Qaidam Basin meteoric water is lower 4.4 [24], which is less than that of gypsum hydration water in Core SG-1. This suggested that brine in the 2.2–0.1 Ma had lighter isotopes than today's local meteoric water and that evaporation was weaker than today's.

## 2.4 Paleoclimatic implications

The climate in the area indicates a long-term persistent aridification event in inland Asia, which is supported by several climate proxies [10–15]. The $\delta^{18}O$ and $\delta D$ of the clay interlayer water and gypsum hydrated water both reflect the compositional variations of the lake water or pore water and record changes in environment [14, 18]. According to the significant positive relationship between $\delta^{18}O$ and $\delta D$ and their low slope (2.933, **Figure 7**), most of the interlayer water could be from pore water and lake water in an evaporative environment. The main factor contributing to the variations in the $\delta^{18}O$ and $\delta D$ water was probably E/P value oscillations, which were linked to the climate changes.

Both the lake water and gypsum hydrated water, their curves of the $\delta^{18}O$ and $\delta D$, display a stepwise increasing trend (**Figure 8**), indicating a drying trend from 2.2 to 0.1 Ma. This is consistent with the global cooling trend, which is also recorded by the $\delta^{18}O$ of marine sediments (**Figure 8**). The lower values of $\delta^{18}O$ and $\delta D$ in 1.2–0.1 Ma than in 2.77–1.2 Ma (**Figure 8**) agreed with the sedimentary changes from brackish lakes to saline and playa lakes [10]. Compared with brackish lakes, it is harder for brines in mudflat and playa lakes to lose water. The occurrence of $Na_2SO_4$-bearing salt minerals such as glauberite, thenardite, mirabilite, and bloedite [11] and the high $\delta^{18}O$ of carbonates [13] also suggest the climate to be extremely
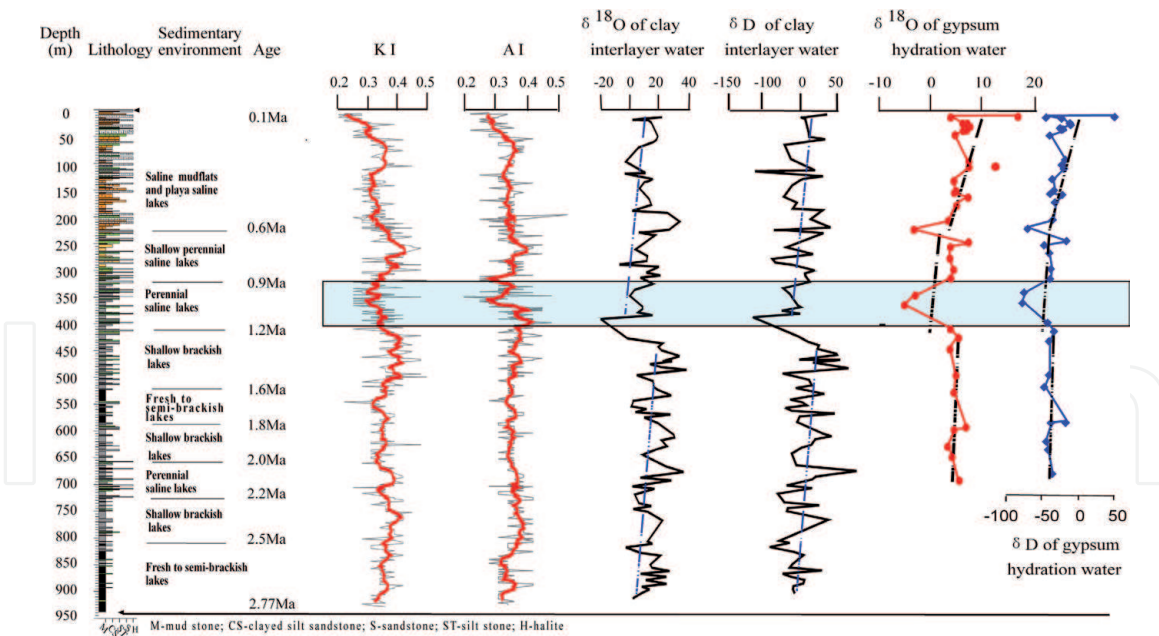
**Figure 8.**
*Hydrogen and oxygen isotopes of gypsum hydrated water and interlayer water of clay minerals vs. depth.*
*The lithologic column and sedimentary environment are from Wang et al. [10]. The ages were based on*
*paleomagnetic results of Zhang et al. [9].*

arid in 1.2–0.1 Ma. At about 1.2–1.1 Ma, the low value was likely due to the MPT cold event, which was also recorded in other places in the Qaidam Basin [49]. This is also consistent with other proxies in Central Asia such as lithological and sedimentary records, evaporative minerals, pollen records, grain size, and trace elements [10–13, 49–51].

In summary, $\delta^{18}O$ and $\delta D$ of the gypsum hydrated water, and interlay water of clay in high saline conditions, both have recorded environmental signals.

## 3. The isotopes of Sr, S, and B of halite in saline conditions

Halite is common in evaporite deposits. Today, exploited evaporite deposits are most found in the arid and semiarid deserts of the world (the areas between latitudes 15° and 45° both north and south of the equator). Tectonics, climate, and origins of brine are the prime controls on most evaporite deposits. However, the origins of brine were a big topic. Giant evaporite deposits typically originate from brines with a marine or/and land origin(s), along with varying inputs from deeply circulated meteoric, basinal, and hydrothermal fluids [52]. The isotopes of S, Sr, and B of halite could be very useful in determining the origins of brine. We used well-known accepted methods to analyze halite and the isotopes to distinguish origins of brine for the evaporite deposits in Laos and Southern China.

### 3.1 Geological setting and the Core ZK2893

#### 3.1.1 Geological setting in Laos and Southern China

Southeast Asia is composed of a series of Gondwana-derived continental blocks which experienced heterogeneous collision with the closure of multiple Tethyan Ocean branches (see reviews in Metcalfe [53, 54]). The Khorat Basin (KB) in Thailand and Sakhon Nakhon Basin (SNB) and the Lanping-Simao Basin (LSB) in Southwest China belong to the Indochina Block (**Figure 9**). The central part of the
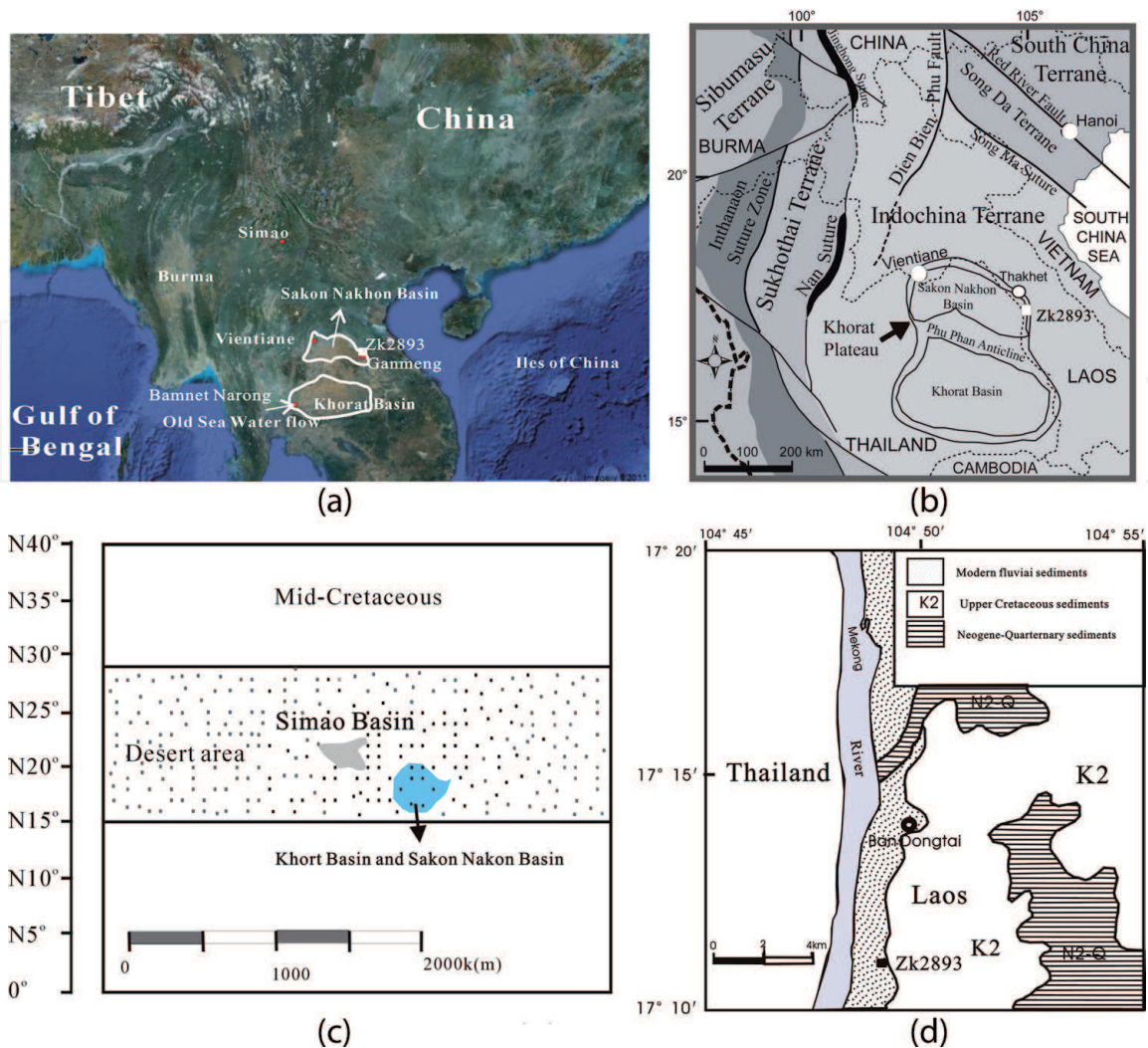
**Figure 9.**
*(a) Google Earth map showing the locations of the Sakhon Nakhon Basin and the Khorat Basin; (b) tectonic map modified from Sone and Metcalfe [55] and El Tabakh et al. [56]; (c) location of Khorat Basin and Sakhon Nakhon Basin, in the Middle and Late Cretaceous (after El Tabakh et al. [56]); (d) geological map showing the general distribution of sediments in the study region (after Zhang et al. [57]).*

Indochina Block (the Khorat Plateau) is relatively rigid with respect to the Simao Terrane (including the LSB) and has been experiencing clockwise rotation of about 15° up to the present day [58, 59]. The location of LSB changed from 25.7° N in Cretaceous to 18.6°N in Paleocene and Eocene [60]. This suggested that the LSB was gradually southward approaching the KB and SNB.

During the Middle and Late Cretaceous, salts formed; however, these salt formations lie atop thick nonmarine sediments of the Mesozoic Khorat Group. The nonmarine sediments were more than 5 km thick, which were deposited in the Late Triassic [56, 61, 62]. From the very Late Triassic to the Early Cretaceous, the KB and SNB were filled with fluvial and lacustrine facies [56]. Due to the occurrence of similar salt minerals within the same tectonic belt in KB and the LSB, they have formed in brines from similar sources [63].

In the mid-Cretaceous, the basins (LSB, KB, and SNB) were within the subtropical high-pressure belt [64]. However, the scale of the Mengye potash deposit in the LSB is much smaller than those in the KB and SNB of Thailand and Laos [63]. This surprising contrast drove many scientists to explore it in the area for ~50 years. But no consensus has therefore been reached regarding their fluid origins [56, 65, 66].

### 3.1.2 The Core ZK2893 in Laos

The lithostratigraphy contained three evaporite-clastic cycles, upper member (148.4 m to top), middle member (299.2–148.4 m), and lower member cycles (595.4–299.2 m), which are composed of evaporite unit and red-colored siliciclastic unit (**Figure 10**). The lithostratigraphy of the core could match with a reviewed section by El Tabakh et al. [56]. Blocky halite beds were only present in the lower and middle members (**Figure 11**). Chevron or cumulate crystals were well developed. Some thin salt units are observed (**Figure 10**), suggesting salt dissolution to be happened and their dissolved solutes to be mixed with their adjacent mudstone. Salt dissolution resulted in a lack of salts in many cores and the deposition of anhydrite [56].

## 3.2 Halite

The evaporite minerals in the halite beds are pure, massive red halite in ZK2893 (**Figure 11**). Some samples have trace or minor anhydrite content [60]. Compared with gypsum, the crystal shapes of halite seldom vary. But halite is much easier to be dissolved and recrystallized than gypsum. The halite crystals in the Core ZK2893 were primary, because (a) the primary fluid inclusions were developed (**Figure 12**), suggesting the halite was not dissolved; (b) the curve of Br in the core changed with depth (**Figure 13C**), consistent with the Br curve of primary halite (**Figure 13A**) and very different with the Br curve of secondary halite (**Figure 13B**); and (c) the Br of basal halite was the lowest in the core, suggesting the primary halite to have been preserved.

Basal halite is defined as the first Cl mineral to be precipitated during the evaporation of seawater/lake water. During syndepositional and early diagenetic processes, Br content of basal halite is stable [69, 71], and the initial compositions of
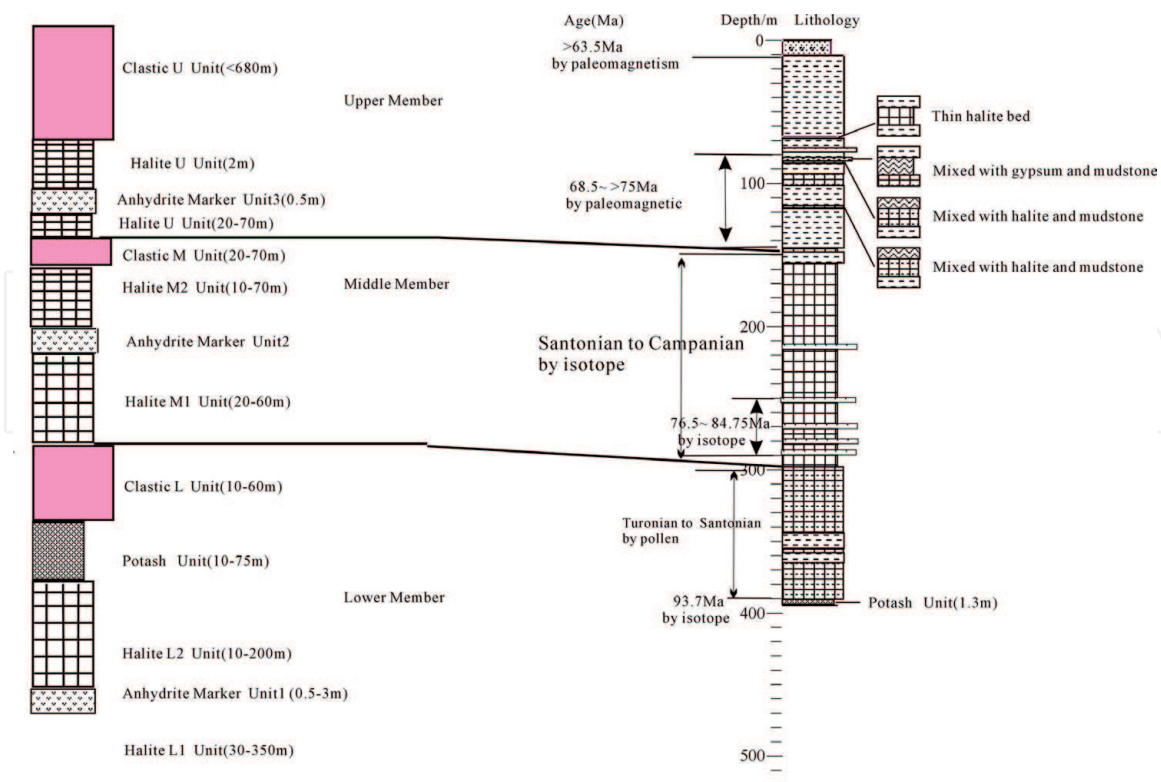


**Figure 10.**
*Left: lithostratigraphical review of the evaporite formation of the Khorat basin and Sakhon Nakhon Basins, after El Tabakh et al. [56]. Right: lithostratigraphy of Core ZK2893 (this study). The paleomagnetic ages are from Zhang [67]; the pollen ages are from Zhong et al. [62]; the isotopic ages are from Hansen et al. [68].*

**Figure 11.**
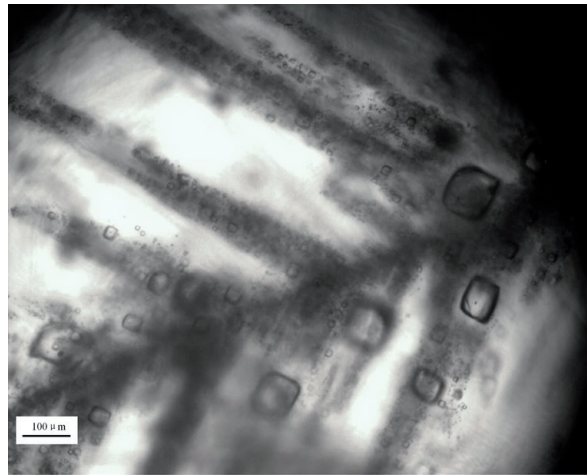*Photos of halite in Core ZK2893 (after Li et al. [60]).*



**Figure 12.**
*Photomicrographs showing primary fluid inclusion banding in chevron halite.*

brine are well-preserved in basal halite [60, 71]. Therefore, the Br content of basal halite can be used to reconstruct the composition and origins of paleo-water. For example, Siemann [71] used the Br content of primary basal halite to reconstruct the Br variations in seawater over the past 500 Ma.

## 3.3 The isotopes of sulfur, strontium, and boron

Isotopic compositions of sulfur, boron, and strontium could be more robust indicators of the origins of evaporites (marine vs. continental origins).

### 3.3.1 Sulfur isotope

Waters from continental sources in general have lower $\delta^{34}S$ values than those from contemporary seawater. The $^{34}S$ values of freshwater usually range from −5 to 5%, while that of recent seawater is globally uniform with value being 20 ± 0.5% [72]. Sulfate minerals (such as gypsum and anhydrite) have stable $\delta^{34}S$ values and are typically resistant to diagenetic alteration [72–74]. Factors influencing the $\delta^{34}S$ values of evaporative sulfates are marine and nonmarine contributions, reservoirs, and redox [72, 74]. For example, bacterial-facilitated sulfate reduction is preferentially enriched in lighter $^{32}S$ isotope, and therefore, the residual sulfate minerals
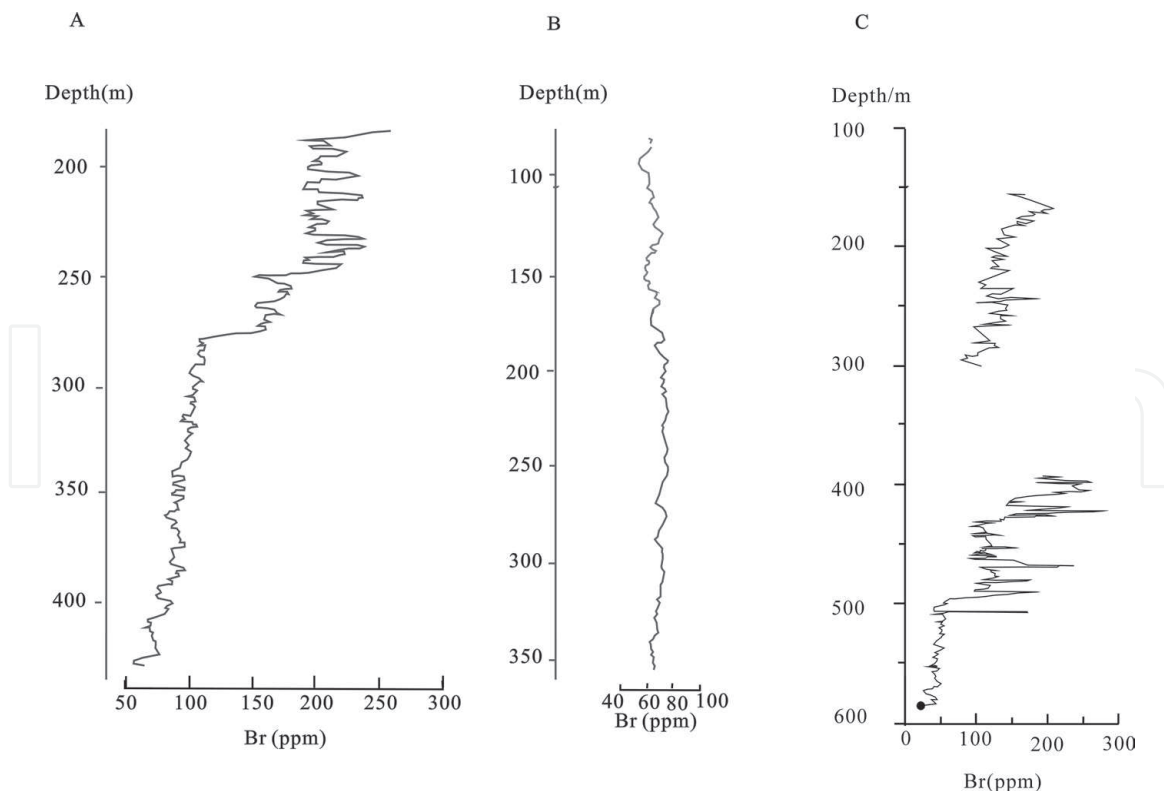
**Figure 13.**
*(A) Curves of Br in primary halite in KB, after Hite and Japakasetr [69]. (B) Curves of Br in secondary halite, after Hite and Japakasetr [69]. (C) Curves of Br in the Core ZK2893 in SNB, Laos [70], suggesting the halite in the core to be primary.*

(such as gypsum) will enrich heavy $^{34}S$ [72, 73]. In contrast, reservoir effects can decrease $\delta^{34}S$ values of the subsequently precipitated gypsum. If sulfate evaporites precipitated in a closed system, the $\delta^{34}S$ values expectedly display a gradual decrease upward in a vertical stratigraphic sequence. The reservoir effect played an active role influencing the $\delta^{34}S$ values of gypsum, anhydrite, and halite in the abovementioned basins (**Figure 14**).

The average of $\delta^{34}S$ values increase from the lower to the upper member, which indicates an evaporation effect. Microbial effect on the core's $\delta^{34}S_{-SO4}$ values may be insignificant. This could be understood in the following. (a) There is no relationship between sulfate concentrations and the $\delta^{34}S_{-SO4}$ values of halite (**Figure 14**). Generally, microbial sulfate reduction can result in an inverse correlation of them [78]. And (b) the $\delta^{34}S$ values observed in the halite and anhydrite are very similar. Redox recycling of bacterial reduction can result in the enrichment of $\delta^{34}S$ values and significant difference within evaporites [72, 73]. Therefore, $\delta^{34}S$ in this study could be used to identify the origins of brine. In the Core ZK2893, all of $\delta^{34}S$ values are lower than, or similar to, those of contemporary seawater (**Figure 14**), suggesting a possible continental origin. Both the $\delta^{34}S$ and $\delta^{18}O_{-SO4}$ values of halite are lower than those of Middle Cretaceous seawater (**Figure 14**) with a short range dispersion, shorter than that between $\delta^{34}S$ and $SO_4$ values (**Figure 14**), suggesting that paleo-lake water possible to be mixed with freshwater.

*3.3.2 Strontium isotope*

Strontium is a divalent alkaline earth element. Its isotope composition is almost homogeneous with modern seawater with $^{87}Sr/^{86}Sr$ values of 0.709175–0.709235 [79, 80]. Because the Sr composition/isotope ratios for the weathering and erosion of rocks are high [81], the $^{87}Sr/^{86}Sr$ ratios for river water evince a large range

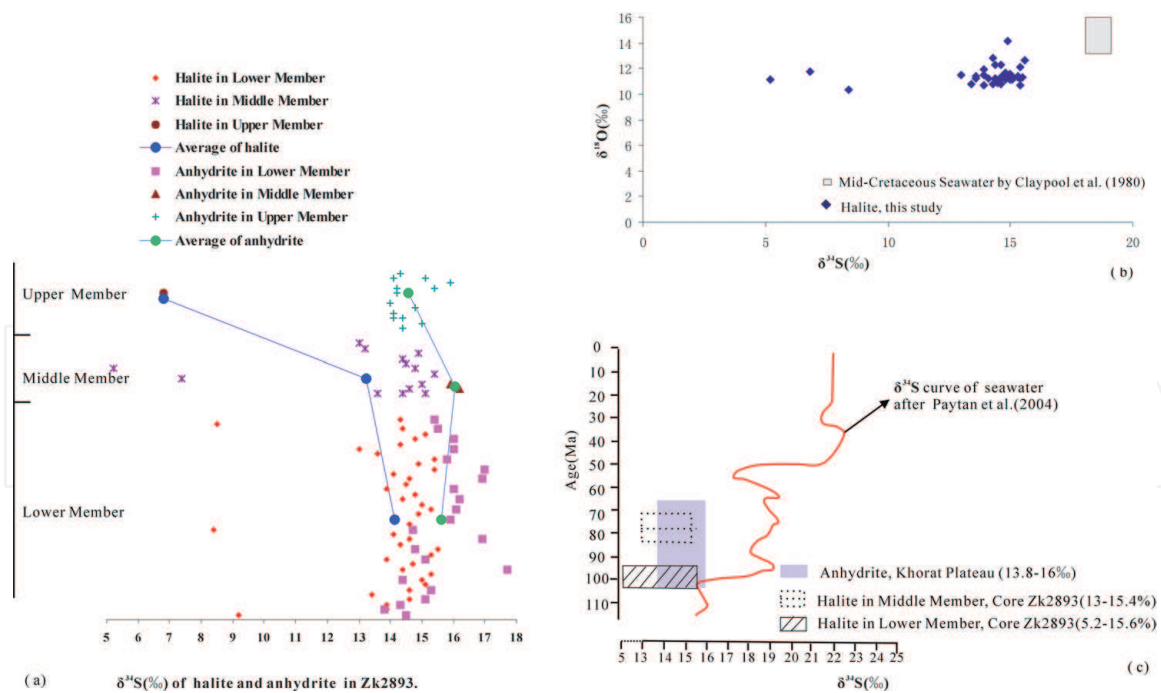**Figure 14.**
*(a) $\delta^{34}S$ values of halite for Core ZK2893 and anhydrite. Anhydrite data are from El Tabakh et al. [58] and Xu [75]. (b) Plot of $\delta^{34}S$-$\delta^{18}O_{-SO_4}$ of halite and Mid-Cretaceous seawater. Mid-Cretaceous seawater data are from Claypool et al. [76]. (c) Comparison of $\delta^{34}S$ values between halite in this study and seawater. The $\delta^{34}S$ curve of seawater from Paytan et al. [77].*

from 0.7074 to 0.803 (**Figure 15**). In a continental setting, the $^{87}Sr/^{86}Sr$ ratio for continental waters is almost always higher than that for marine waters (**Figure 15**). The $^{87}Sr/^{86}Sr$ values of Paleocene halite in the Qaidam Basin (a continental basin), for example, were higher than those of Paleocene seawater (**Figure 9**). Thus, the $^{87}Sr/^{86}Sr$ values of authigenic minerals are very variable and higher than those of seawater when the minerals are precipitated from a solution.

As no fractionation of Sr isotopes occurs during halite precipitation, the measured halite $^{87}Sr/^{86}Sr$ ratios for Core ZK2893 (ranging from 0.707443 to 0.708587) could represent those of the parent solution. $^{87}Sr/^{86}Sr$ ratios for the lower member ranged from 0.707443 to 0.708587, averaging 0.707693, while those for the middle member ranged from 0.70752 to 0.708105, averaging 0.70764. There was only one $^{87}Sr/^{86}Sr$ ratio value in the upper member, of 0.708163. In the lower member, the possible reasons for the high $^{87}Sr/^{86}Sr$ ratios in the upper part (**Figure 15**) are (a) the permeation of continental waters from the middle clastic unit into the halite layers and (b) an inflow of continental waters into the Sakhon Nakhon Basin during the shrinkage process of the basin. However, the $^{87}Sr/^{86}Sr$ ratios exhibit no significant variability in the middle member [83], suggesting no, or little, penetration of continental waters into the halite layers. The $^{87}Sr/^{86}Sr$ and 1/Sr halite ratios in Core ZK2893 do not show a linear relation but rather a weak positive relation (**Figure 15a**). Some $^{87}Sr/^{86}Sr$ ratios are far higher than those of contemporary seawater, indicating the possible input of continental waters into these evaporite basins; these $^{87}Sr/^{86}Sr$ ratios in the lower member are lower than, or similar to, those of Cretaceous seawater; further, mean Middle Cretaceous $^{87}Sr/^{86}Sr$ ratios are similar to those of paleo-seawater (**Figure 15b**), suggesting a marine remnant origin.

### 3.3.3 Boron isotope

Natural boron, a highly soluble element, has two stable isotopes ($^{10}B$ and $^{11}B$) with approximate abundances of 20 and 80%, respectively. Boron isotope
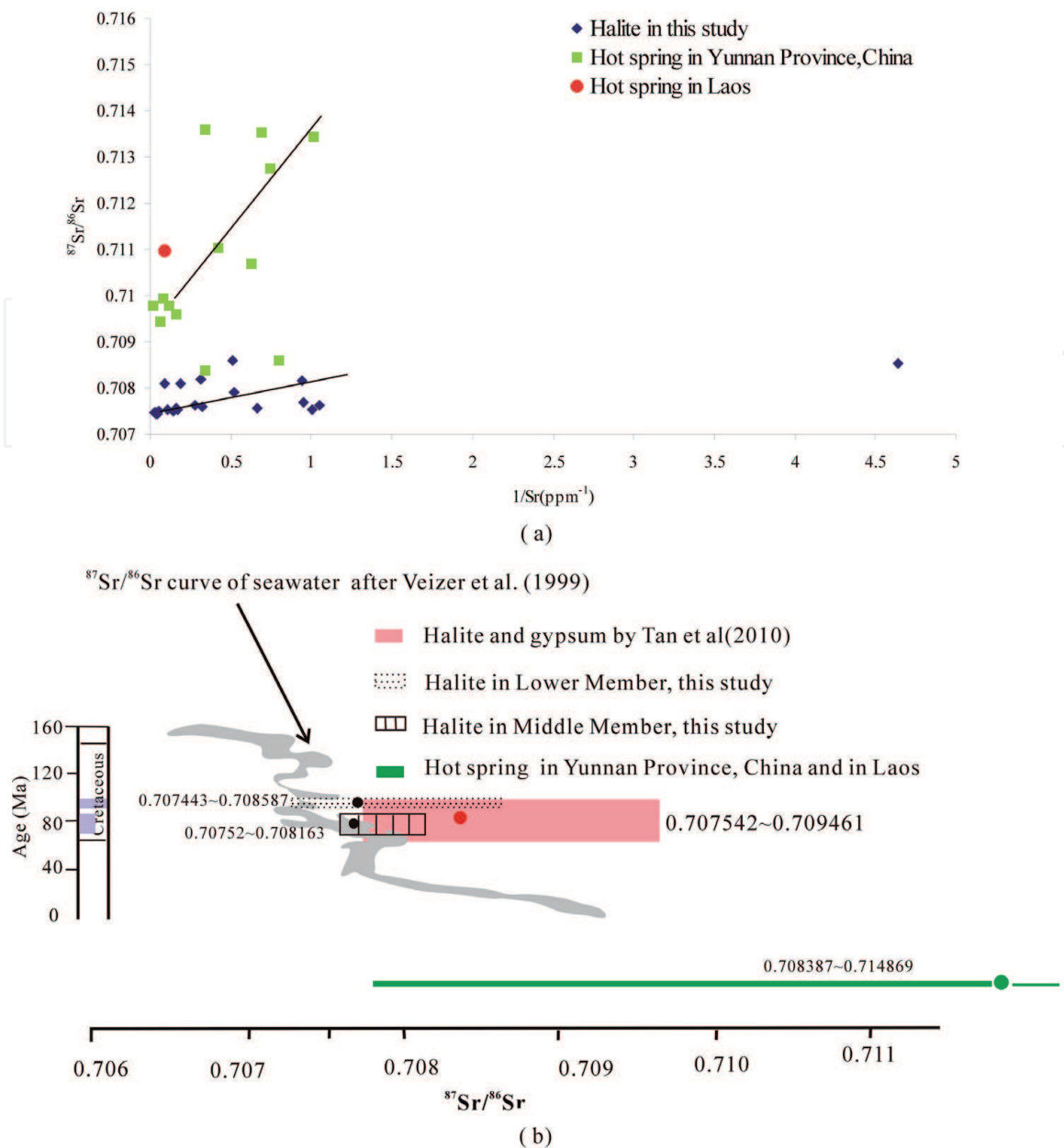
**Figure 15.**
*(a) Plot of $^{87}Sr/^{86}Sr$ and $1/Sr$ of halite and hot spring water; and (b) $^{87}Sr/^{86}Sr$ ratios in halite, gypsum, hot spring water and saline lake water: A dot indicates a mean value. Gypsum data are from Tan et al. [66], hot spring data for Yunnan Province in China, and for Laos, are from Bo et al. [82].*

fractionation is dependent upon the distribution of boron species, temperature, and pH, but pH is the key factor [84–89]. Dissolved boron exists mainly in the form of $B(OH)_3$ and $B(OH)_4$, which are dominantly present as $^{11}B(OH)_3$ at low pH values and as $^{10}B(OH)_4$ at high pH values [85–88]. Because pH values increased with the increasing extent of evaporation, the minerals precipitated in early stages have higher $\delta^{11}B$ values than those of minerals precipitated in later stages. Generally, the sequence of $\delta^{11}B$ values of different minerals is following as: carbonate > gypsum > borate > halite > sylvite. As boron was present in inclusion [90], the $\delta^{11}B$ values of halite and sylvite are exactly representative of those for contemporary paleo-brines. Therefore, the $\delta^{11}B$ values of halite and sylvite are higher than those in carbonates and borate minerals, and all of minerals have lower $\delta^{11}B$ than those of brine. In the Core ZK2893, however, the $\delta^{11}B$ values of halite and sylvite were lower than those of borate minerals (**Figure 16**). One possible reason is that there have different sources of brines, such as continental, marine residue and groundwater/hydrothermal brine. In the LSB, China, most of $\delta^{11}B$ values of
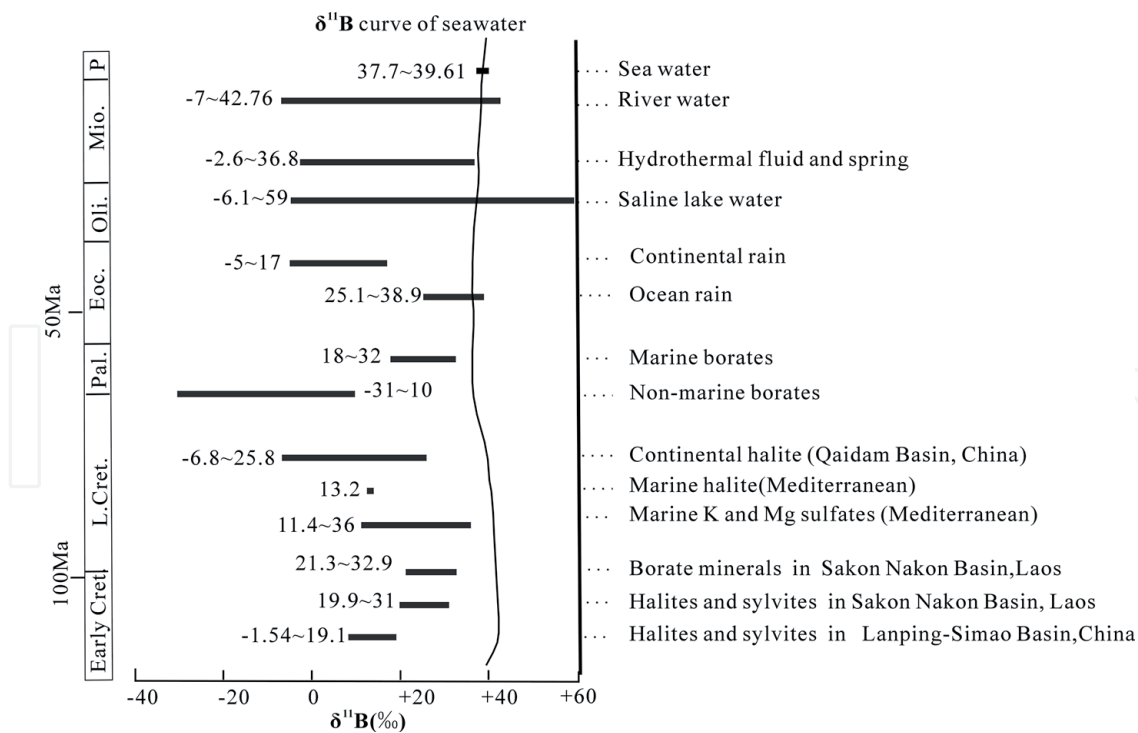
**Figure 16.**
*δ¹¹B values from published papers. Marine and nonmarine borates after Swihart et al. [91], Xiao et al. [90], and Palmer and Helvaci [85]. Seawater after Vengosh et al. [86] and Foster et al. [89]. River water after Vengosh et al. [7]; Rose et al. [92]; and Lemarchand et al. [93]. Halite after from Vengosh et al. [86]; Liu et al. [94]; and Kloppmann et al. [95]. Borate minerals in SNB after Zhang et al. [96]. Halite and sylvite in SNB after Tan et al. [66]). Halite and sylvite in LSB after Zhang et al. [97]. Curve of seawater after Lemarchand et al. [98].*

halite and sylvite ranged from −1.54 to 19.1%, which are lower than those in Laos (19.9–31.1‰) (**Figure 16**). This suggested the paleo-brines in LSB, China, are from Laos and diluted during the flow process.

Comparison of δ¹¹B values between known marine minerals and unknown minerals is a useful way to distinguish marine and continental origin. In nonmarine setting, some δ¹¹B values of hydrothermal fluid, saline lake water and river water, are higher than those of seawater (**Figure 16**), that is, lower δ¹¹B values of minerals than that of seawater are not indicate continental origin. The comparison of δ¹¹B between salt minerals is valid. Although the δ¹¹B values of halite in Laos were lower than those of seawater, they were near to those of marine borates (**Figure 16**). This suggested minor or trace marine origin. The δ¹¹B values of the evaporite in LSB in China are lower than, but some are near to, those of halite and sylvite in SNB, Laos, also suggesting continental origin with minor residual seawater.

In summary, halite isotopic compositions (in the form of $\delta^{34}S$-$\delta^{18}O_{-SO4}$ values, $^{87}Sr/^{86}Sr$ and $\delta^{11}B$) appear to represent an original composition associated with brine. These isotopic proxies indicate that continental and hydrothermal origins are likely to be more important sources of evaporite deposits than marine origins for these Laotian evaporite deposits.

## 4. Summary

The gypsum in the Core SG-1 was deposited directly from brines and was stable after deposition. The $\delta^{18}O$ and $\delta D$ curves of hydrated water in gypsum record the evolution of paelo-lake in Qaidam Basin, Western Tibetan Plateau since 2.2 Ma, including the famous cold event, mid-Pleistocene event.

In high saline conditions, the clay minerals from Core SG-1 may have undergone early diagenesis. The primary illite and chlorite contents in Core SG-1 were lower than those observed, while the primary smectite and kaolinite contents were higher than those observed. After early diagenesis, there were no isotopic exchange between the interlayer water and the ambient water. The $\delta^{18}O$ and $\delta D$ values indicated the interlayer water of clay minerals to be more concentrated than those of hydrated water. The isotopic composition of the interlayer water reflects variations in the pore water/lake water or in the reacting solutions and also records changes in environment.

Using isotopic compositions of salt minerals to identify origins of brine is a complex topic. It should be careful to use sole isotope to identify the origins. For the evaporite deposits in LSB in China and NSB, in Laos, these isotopic proxies, including $\delta^{34}S$-$\delta^{18}O_{-SO4}$, $^{87}Sr/^{86}Sr$, and $\delta^{11}B$, indicate that continental and hydrothermal origins are likely to be more important than marine origins.

## Acknowledgements

## Author details

Minghui Li[1,2*], Xiaomin Fang[2,3,4], Jiao Li[1], Maodu Yan[2,3], Shurui Sun[1] and Liping Zhu[1,2,4]

1 Key Laboratory of Tibetan Environment Changes and Land Surface Processes, Institute of Tibetan Plateau Research, Chinese Academy of Sciences (ITPCAS), Beijing, China

2 CAS Center for Excellence in Tibetan Plateau Earth Sciences, Beijing, China

3 Key Laboratory of Continental Collision and Plateau Uplift, ITPCAS, Beijing, China

4 University of Chinese Academy of Sciences, Beijing, China

*Address all correspondence to: liminghui@itpcas.ac.cn

IntechOpen

## References

[1] Chen K, Bowler JM. Late Pleistocene evolution of salt lakes in the Qaidam basin, Qinghai province, China. Palaeogeography, Palaeoclimatology, Palaeoecology. 1986;**54**:87-104

[2] Qian ZQ, Qu YH, Liu Q, editors. Potash Deposits. Beijing: Geological Press; 1994 (in Chinese)

[3] Fang X, Zhang W, Meng X, Gao J, Wang X, King J, et al. High-resolution magnetostratigraphy of the Neogene Huaitoutala section in the eastern Qaidam Basin on the NE Tibetan Plateau, Qinghai Province, China and its implication on tectonic uplift of the NE Tibetan Plateau. Earth and Planetary Science Letters. 2007;**258**(1-2):293-306

[4] Tuo J, Philp RP. Occurrence and distribution of high molecular weight hydrocarbons in selected non-marine source rocks from the Liaohe, Qaidam and Tarim Basins, China. Organic Geochemistry. 2003;**34**:1543-1558

[5] Liu X, Dong H, Jason AR, Matsumoto R, Yang B, Wang Y. Evolution of Chaka Salt Lake in NW China in response to climatic change during the Latest Pleistocene-Holocene. Quaternary Science Reviews. 2008;**27**:867-879

[6] Mischke S, Sun Z, Herzschuh U, Qiao Z, Sun N. An ostracod-inferred large Middle Pleistocene freshwater lake in the presently hyper-arid Qaidam Basin (NW China). Quaternary International. 2010;**218**:74-85

[7] Vengosh A, Chivas AR, Starinsky A, Kolodny Y, Baozhen Z, Zhang P. Chemical and boron isotope compositions of non-marine brines from the Qaidam Basin, Qinghai, China. Chemical Geology. 1995;**120**:135-154

[8] Eugster HP. Geochemistry of evaporitic lacustrine deposits. Annual Review of Earth and Planetary Sciences. 1980;**8**:35-63

[9] Zhang WL, Appel E, Fang XM, Song CH, Cirpka O. Magnetostratigraphy of deep drilling core SG-1 in the western Qaidam Basin (NE Tibetan Plateau) and its tectonic implications. Quaternary Research. 2012;**78**(1):139-148

[10] Wang JY, Fang XM, Appel E, Song CH. Pliocene-Pleistocene climate change at the NE Tibetan Plateau deduced from lithofacies variation in the drill Core SG-1, western Qaidam basin, China. Journal of Sedimentary Research. 2012;**82**(12):933-952

[11] Li MH, Fang XM, Wang JY, Song YG, Yang YB, Zhang WL, et al. Evaporite minerals of the lower 538.5 m sediments in a long core from the Western Qaidam basin, Tibet. Quaternary International. 2013;**298**:123-133

[12] Li MH, Fang XM, Yi CL, Gao SP, Zhang WL, Galy A. Evaporite minerals and geochemistry of the upper 400 m sediments in a core from the Western Qaidam Basin, Tibet. Quaternary International. 2010;**218**(1-2):176-189

[13] Han WX, Fang XM, Ye CC, Teng XH, Zhang T. Tibet forcing quaternary stepwise enhancement of westerly jet and central Asian aridification: Carbonate isotope records from deep drilling in the Qaidam salt playa, NE Tibet. Global and Planetary Change. 2014;**116**:68-75

[14] Li J, Li MH, Fang XM, Zhang GX, Zhang WL, Liu XM. Isotopic composition of gypsum hydration water in deep Core SG-1, western Qaidam basin (NE Tibetan Plateau), implications for paleoclimatic evolution. Global and Planetary Change. 2017;**155**:70-77

[15] Yang YB, Fang XM, Galy A, Li MH, Appel E, Liu XM. Paleoclimatic significance of rare earth element record of the calcareous lacustrine sediments from a long core (SG-1) in the western Qaidam Basin, NE Tibetan plateau. Journal of Geochemical Exploration. 2014;**145**:223-232

[16] Singer A. The paleoclimatic interpretation of clay minerals in sediments: A review. Earth-Science Reviews. 1984;**21**:251-293

[17] Dong H. Interstratified illite-smectite: A review of contributions of TEM data to crystal chemical relations and reaction mechanisms. Clay Science. 2005;**12**(Suppl. 1):6-12

[18] Li M, Sun S, Fang X, Wang C, Wang Z, Wang H. Clay minerals and isotopes of Pleistocene lacustrine sediments from the western Qaidam Basin, NE Tibetan Plateau. Applied Clay Science. 2018;**162**:382-390

[19] Savin SM, Lee M. Isotopic studies of phyllosilicates. In: Bailey SW, editor. Hydrous Phyllosilicates (Exclusive of Micas). Reviews in Mineralogy. Vol. 19. Washington, DC: Mineralogical Society of America; 1988. pp. 189-224

[20] Inoue A, Meunier A, Beaufort D. Illite-smectite mixed-layer minerals in felsic volcanic lastic rocks from drill cores, Kakkonda, Japan. Clays and Clay Minerals. 2004;**52**(1):66-84

[21] Sánchez-Roa C, Jiménez-Millán J, Abad I, Faulkner DR, Nieto F, García-Tortosa FJ. Fibrous clay mineral authigenesis induced by fluid-rock interaction in the Galera fault zone (Betic Cordillera, SE Spain) and its influence on fault gouge frictional properties. Applied Clay Science. 2016;**134**:275-288

[22] Craig H. Isotopic variations in meteoric waters. Science. 1961;**133**(3465):1702-1703

[23] Li X, Zhang M, Li Y, Wang S, Huang X, Ma Q, et al. Characteristics of δ18O in precipitation and moisture transports over the arid region in Northwest China. Environmental Sciences. 2012;**33**:711-719 (in Chinese with English abstract)

[24] Zhang P. Salt Lake of Qaidam Bain. Beijing: Science Press; 1987. pp. 32-233 (in Chinese)

[25] Fan Q, Ma HZ, Tan HB, Xu JX, Li TW. Characteristics and origins of brines in Western Qaidam Basin. Geochimica. 2007;**36**(6):633-637

[26] Xiao Y. Oxygen and hydrogen isotope research of different waters in Qarhan salt lake and lake sediments. Journal of Xiamen University (Natural Science). 1995;**34**(2):255

[27] James AT, Baker DR. Oxygen isotope exchange between illite and water at 22°C. Geochimica et Cosmochimica Acta. 1976;**40**:235-239

[28] O'Neil JR, Kharaka YK. Hydrogen and oxygen isotope exchange reactions between clay minerals and water. Geochimica et Cosmochimica Acta. 1976;**40**:241-246

[29] Zheng YF, Chen JF. Stable Isotope Geochemistry. Beijing: Science Publishing House; 2000. pp. 218-247 (in Chinese)

[30] Li J, Li MH, Fang XM, Wang ZR, Zhang WL, Yang YB. Variations and mechanisms of gypsum morphology along deep core SG-1, western Qaidam Basin (northeastern Tibetan Plateau). Quaternary International. 2017;**430**:71-81

[31] Warren JK. Evaporites brines and base metals: What is an evaporite? Defining the rock matrix. Australian Journal of Earth Sciences. 1996;**43**:115-132

[32] Gibert L, Ortí F, Rosell L. Plio-pleistocene lacustrine evaporites of the Baza Basin (Betic Chain, SE Spain). Sedimentary Geology. 2007;**200**:89-116

[33] Mees F, Casteneda C, Herrero J, Ranst EV. The nature and significance of variations in gypsum crystal morphology in dry lake basins. Journal of Sedimentary Research. 2012;**82**:37-52

[34] Hodell DA, Turchyn AV, Wiseman CJ, Escobar J, Curtis JH, Brenner M, et al. Late glacial temperature and precipitation changes in the lowland Neotropics by tandem measurement of δ18O in biogenic carbonate and gypsum hydration water. Geochimica et Cosmochimica Acta. 2012;**77**:352-368

[35] Evans NP, Turchyna AV, Gázquez F, Bontognali TRR, Chapman HJ, Hodell DA. Coupled measurements of δ18O and δD of hydration water and salinity of fluid inclusions in gypsum from the Messinian Yesares Member, Sorbas Basin (SE Spain). Earth and Planetary Science Letters. 2015;**430**:499-510

[36] Khademi H, Mermut AR, Krouse HR. Isotopic composition of gypsum hydration water in selected landforms from central Iran. Chemical Geology. 1997;**138**(3):245-255

[37] Cody RD. Organo-crystalline interactions in evaporite systems: The effects of crystallization inhibition. Journal of Sedimentary Research. 1991;**61**:704-718

[38] Magee JW. Late quaternary lacustrine, groundwater, aeolian and pedogenic gypsum in the Prungle Lakes, southeastern Australia. Palaeogeography, Palaeoclimatology, Palaeoecology. 1991;**84**:3-42

[39] Edinger SE. An investigation of the factors which affect the size and growth rates of the habit faces of gypsum. Journal of Crystal Growth. 1973;**18**:217-224

[40] Zhang J, Nancollas GH. Influence of calcium/sulfate molar ratio on the growth rate of calcium sulfate dihydrate at constant supersaturation. Journal of Crystal Growth. 1992;**118**:287-294

[41] Franchini-Angela M, Rinaudo C. Influence of sodium and magnesium on the growth-morphology of gypsum, $CaSO_4$. $2H_2O$. Neues Jahrbuch Fur Mineralogie Abhandlungen. 1989;**160**:105-115

[42] Wang ML, Yang ZC, Liu CL, Xie ZC, Jiao PC, Li CH. Potash Deposits and Their Exploitation Prospects of Saline Lakes of the Northern Qaidam Basin. Beijing: Geological Publishing House; 1996. pp. 33-51 (in Chinese)

[43] Farpoor MH, Khademi H, Eghbal MK, Krouse HR. Mode of gypsum deposition in southeastern Iranian soils as revealed by isotopic composition of crystallization water. Geoderma. 2004;**121**(3-4):233-242

[44] Sofer Z. Isotopic composition of hydration water in gypsum. Geochimica et Cosmochimica Acta. 1978;**42**(8):1141-1149

[45] Dowuona GN, Mermut AR, Krouse HR. Isotopic composition of hydration water in gypsum and hydroxyl in jarosite. Soil Science Society of America Journal. 1992;**56**(1):309-313

[46] Matsubaya O, Sakai H. Oxygen and hydrogen isotopic study on the water of crystallization of gypsum from the Kuroko type mineralization. Geochemical Journal. 1973;**7**(3):153-165

[47] Chen F, Turchyn AV, Kampman N, Hodell D, Gázquez F, Maskell A, et al. Isotopic analysis of sulfur cycling and gypsum vein formation in a natural $CO_2$ reservoir. Chemical Geology. 2016;**436**:72-83

[48] Sofer Z, Gat JR. The isotope composition of evaporating brines: Effect of the isotopic activity ratio in saline solutions. Earth and Planetary Science Letters. 1975;**26**(2):179-186

[49] Cai MT, Fang XM, Wu FL, Miao YF, Appel E. Pliocene-Pleistocene stepwise drying of Central Asia: Evidence from paleomagnetism and sporopollen record of the deep borehole SG-3 in the western Qaidam Basin, NE Tibetan Plateau. Global and Planetary Change. 2012;**94-95**:72-81

[50] Wu FL, Fang XM, Ma YZ, Herrmann M, Mosbrugger V, An ZS, et al. Plio–Quaternary stepwise drying of Asia: Evidence from a 3-Ma pollen record from the Chinese Loess Plateau. Earth Planetary Science Letters. 2007;**257**(1-2):160-169

[51] Ding ZL, Sun JM, Liu DS. Stepwise advance of the Mu Us desert since late Pliocene: Evidence from a red clay-loess record. Chinese Science Bulletin. 1999;**44**:1211-1214

[52] Warren JK. Evaporites: Sediments, Resources and Hydrocarbons. Berlin: Springer; 2006

[53] Metcalfe I. Tectonic framework and Phanerozoic evolution of Sundaland. Gondwana Research. 2011;**19**:3-21

[54] Metcalfe I. Gondwana dispersion and Asian accretion: Tectonic and palaeogeographic evolution of eastern Tethys. Journal of Asian Earth Sciences. 2013;**66**:1-33

[55] Sone M, Metcalfe I. Parallel Tethyan sutures in mainland Southeast Asia: New insights for Palaeo-Tethys closure and implications for the Indosinian orogeny. Comptes Rendus Geoscience. 2008;**340**(2-3):166-179

[56] El Tabakh M, Utha-Aroon C, Schreiber BC. Sedimentology of the Cretaceous Maha Sarakham evaporites in the Khorat Plateau of northeastern Thailand. Sedimentary Geology. 1999;**123**(1-2):31-62

[57] Zhang XY, Ma HZ, Tan HB, Gao DL, Li BK, Wang MX, et al. Preliminary studies of on geochemistry and post-depositional change of Dong Tai potash deposit in Laos. Mineral Deposits. 2010;**4**:713-721

[58] Yang ZY, Besse J. Paleomagnetic study of Permian and Mesozoic sedimentary rocks from Northern Thailand supports the extrusion model for Indochina. Earth and Planetary Science Letters. 1993;**117**:525-552

[59] Yang W, Spencer RJ, Roy Krouse H, Lowenstein TK, Casas E. Stable isotopes of lake and fluid inclusion brines, Dabusun Lake, Qaidam Basin, western China: Hydrology and paleoclimatology in arid environments. Palaeogeography Palaeoclimatology Palaeoecology. 1995;**117**:279-290

[60] Li MH, Yan MD, Wang ZR, Liu XM, Fang XM, Li J. The origins of the Mengye potash deposit in the Lanping-Simao Basin, Yunnan Province, Western China. Ore Geology Reviews. 2015;**69**:174-186

[61] Timofeeff MN, Lowenstein TK, Da Silva MAM, Harris NB. Secular variation in the major-ion chemistry of seawater: Evidence from fluid inclusions in cretaceous halites. Geochimica et Cosmochimica Acta. 2006;**70**(8):1977-1994

[62] Zhong XY, Yuan Q, Qin ZJ, Wei HC, Shan FS. The sporo-pollen analyses and ore-forming age of Nong Bok formation in Khammouane, Laos. Acta Geoscientica Sinica. 2012;**33**(3):323-330 (in Chinese with English abstract)

[63] Qu YH, Yuan PQ, Shuai KY, Zhang Y, Cai KQ, Jia SY, et al. Potash Forming Rules and Prospects of Lower Tertiary in Lanping-Simao Basin,

Yunnan. Beijing: Geological Press; 1998 (in Chinese with English abstract)

[64] Hasegawa H, Imsamut S, et al. Thailand was a desert' during the mid-Cretaceous: Equatorward shift of the subtropical high-pressure belt indicated by Eolian deposits (Phu Thok Formation) in the Khorat Basin, northeastern Thailand. Island Arc. 2010;**19**(4):605-621

[65] Utha-Aroon C. Continental origin of the Maha Sarakham evaporites, northeastern Thailand. Journal of Southeast Asian Earth Sciences. 1993;**8**(1-4):193-203

[66] Tan H, Ma H, Li BK, Zhang XY, Xiao YK. Strontium and boron isotopic constraint on the marine origin of the Khammouane potash deposits in southeastern Laos. Chinese Science Bulletin. 2010;**55**(27):3181-3188

[67] Zhang DW. Magnetostratigraphic studies of the Potash-bearing strata of the Lanping-Simao and the Vientiane Basins and their tectonic implications [thesis]. University of Chinese Academy of Sciences; 2016 (in Chinese with English abstract)

[68] Hansen BT, Wemmer K, Pawlig S, et al. Isotopic evidence for a Late Cretaceous age of the potash and rock salt deposit at Bamnet Narong, NE Thailand. In: Symposium on the Geology of Thailand, Bangkok; August 2002; Extended Abstract; 2002. pp. 26-31

[69] Hite RJ, Japakasetr T. Potash deposits of the khorat plateau, Thailand and Laos. Economic Geology. 1979;**74**(2):448-458

[70] Sun SR, Li MH, Yan MD, Fang XM, Zhang GX, Liu XM. et al. Bromine content and Br/Cl molar ratio of halite in a core from Laos: Implications for origin and environmental changes. Carbonates and Evaporites. 2019. DOI: 10.1007/s13146-019-00508-0

[71] Siemann MG. Extensive and rapid changes in seawater chemistry during the Phanerozoic: Evidence from Br contents in basal halite. Terra Nova. 2003;**15**(4):243-248

[72] Lu FH, Meyers WJ, Schoonen MA. S and O ($SO_4$) isotopes, simultaneous modeling, and environmental significance of the Nijar Messinian gypsum, Spain. Geochimica et Cosmochimica Acta. 2001;**65**(18):3081-3092

[73] Pierre C. Isotopic evidence for the dynamic redox cycle of dissolved sulphur compounds between free and interstitial solutions in marine salts pans. Chemical Geology. 1985;**53**:191-196

[74] Bottrell SH, Newton RJ. Reconstruction of changes in global sulfur cycling from marine sulfate isotopes. Earth Science Reviews. 2006;**75**:59-83

[75] Xu JX. Geochemistry and genesis of Mengyejing potash deposits [thesis]. Yunnan: Chinese Academy Science; 2008 (in Chinese with English abstract)

[76] Claypool GE, Holser WT, Kaplan IR, Sakai H, Zak I. The age curves of sulfur and oxygen isotopes in marine sulfate and their mutual interpretation. Chemical Geology. 1980;**28**:199-260

[77] Paytan A, Kastner M, Campbell D, Thiemens MH. Seawater sulfur isotope fluctuations in the Cretaceous. Science. 2004;**304**:1663-1665

[78] Hurtgen MT, Suits NS, Kaufman AJ. The sulfur isotopic composition of Neoproterozoic seawater sulfate: Implications for a snowball earth? Earth and Planetary Science Letters. 2002;**203**(1):413-429

[79] Hess J, Bender ML, Schilling JG. Evolution of ratio of strontium 87 to strontium 86 in seawater from

cretaceous to present. Science. 1986;**231**:979-984

[80] Krabbenhöft A, Eisenhauer A, Böhm F, Vollstaedt H, Fietzke J, Liebetrau V, et al. Constraining the marine strontium budget with natural strontium isotope fractionations (87Sr/86Sr, δ88/86Sr) of carbonates, hydrothermal solutions and river waters. Geochimica et Cosmochimica Acta. 2010;**74**:4097-4109

[81] Rahaman W, Singh SK, Sinha R, Tandon SK. Sr, C and O isotopes in carbonate nodules from the Ganga Plain: Evidence for recent abrupt rise in dissolved 87Sr/86Sr ratios of the Ganga. Chemical Geology. 2011;**285**:184-193

[82] Bo Y, Liu CL, Zhao YJ, Wang LC. Chemical and isotopic characteristics and origin of spring waters in the Lanping-Simao Basin, Yunnan, Southwestern China. Chemie der Erde-Geochemistry. 2015;**75**:287-300

[83] Li MH, Yan MD, Fang XM, Zhang ZJ, Wang ZR, Sun SR, et al. Origins of the Mid-Cretaceous evaporite deposits of the Sakhon Nakhon Basin in Laos: Evidence from the stable isotopes of halite. Journal of Geochemical Exploration. 2018;**184**:209-222

[84] Spivack AJ, Edmond JM. Boron isotope exchange between seawater and the oceanic-crust. Geochimica et Cosmochimica Acta. 1987;**51**(5):1033-1043

[85] Palmer MR, Helvaci C. The boron isotope geochemistry of the neogene borate deposits of western Turkey. Geochimica et Cosmochimica Acta. 1997;**61**(15):3161-3169

[86] Vengosh A, Starinsky A, Kolodny Y, Chivas AR, Raab M. Boron isotope variations during fractional evaporation of sea water: New constraints on the

marine vs. nonmarine debate. Geology. 1992;**20**:799-802

[87] Pagani M, Lemarchand D, Spivack A, Gaillardet J. A critical evaluation of the boron isotope-pH proxy: The accuracy of ancient ocean pH estimates. Geochimica et Cosmochimica Acta. 2005;**69**(4):953-961

[88] Paris G, Gaillardet J, Louvat P. Geological evolution of seawater boron isotopic composition recorded in evaporites. Geology. 2010;**38**(11):1035-1038

[89] Foster GL, Pogge von Strandmann PAE, et al. Boron and magnesium isotopic composition of seawater. Geochemistry, Geophysics, Geosystems. 2010;**11**(8):Q08015

[90] Xiao Y, Sun D, Wang YH, Qi HP, Jin L. Boron isotopic compositions of brine, sediments, and source water in Da Qaidam Lake, Qinghai, China. Geochimica et Cosmochimica Acta. 1992;**56**:1561-1568

[91] Swihart GH, Moore PB. Boron isotopic composition of marine and nonmarine evaporite borates. Geochimica et Cosmochimica Acta. 1986;**50**(6):1297-1301

[92] Rose EF, Chaussidon M, France-Lanord C. Fractionation of boron isotopes during erosion processes: The example of Himalayan rivers. Geochimica et Cosmochimica Acta. 2000;**64**(3):397-408

[93] Lemarchand D, Gaillardet J, Lewin E. Boron isotope systematics in large rivers: Implications for the marine boron budget and paleo-pH reconstruction over the Cenozoic. Chemical Geology. 2002;**190**(1):123-140

[94] Liu WG, Xiao YK, Peng ZC, An ZS, He XX. Boron concentration and isotopic composition of halite from experiments and

salt lakes in the Qaidam Basin. Geochimica et Cosmochimica Acta. 2000;**64**(13):2177-2183

[95] Kloppmann W, Négrel P, Casanova J, Klinge H, Schelkes K, Guerrot C. Halite dissolution derived brines in the vicinity of a Permian salt dome (N German Basin). Evidence from boron, strontium, oxygen, and hydrogen isotopes. Geochimica et Cosmochimica Acta. 2001;**65**(22):4087-4101

[96] Zhang X, Ma H, Ma YQ, Tang QL, Yuan XL. Origin of the late Cretaceous potash-bearing evaporites in the Vientiane Basin of Laos: δ11B evidence from borates. Journal of Asian Earth Sciences. 2013;**62**(0):812-818

[97] Zhang CW, Gao DL, Zhang SY, Tang QL, Shi L. Comparison of geochemistry characteristics in Palaeocene salt-bearing strata of Lanping-Simao Basin and Chuxiong Basin. Journal of the Salt Lake Research. 2011;**19**(3):8-14 (in Chinese with English abstract)

[98] Lemarchand D, Gaillardet J, Lewin EÂ, AlleÂgre CJ. The influence of rivers on marine boron isotopes and implications for reconstructing past ocean pH. Nature. 2000;**408**:951-954